



Species-specific differential dissolution morphology of selected coccolithophore species: an experimental study

Gerald Langer^{1,2}, Ian Probert³, Jeremy R. Young⁴, and Patrizia Ziveri^{1,5,6}

¹Institute of Environmental Science and Technology, Universitat Autònoma de Barcelona (ICTA-UAB), Barcelona, 08193, Spain

²Marine Biogeosciences, Alfred Wegener Institute, Helmholtz-Zentrum für Polar- und Meeresforschung, 27570 Bremerhaven, Germany

³Sorbonne Université/CNRS, Roscoff Culture Collection, FR2424 Station Biologique de Roscoff, 29682 Roscoff, France

⁴Earth Sciences, University College London, London WC1E 6BT, UK

⁵Catalan Institution for Research and Advanced Studies (ICREA), Barcelona, Spain

⁶Department of Animal Biology, Plant Biology and Ecology (BABVE), Universitat Autònoma de Barcelona, Bellaterra, Spain

Correspondence: Gerald Langer (gerald.langer@cantab.net, gerald.langer@awi.de)

Received: 24 April 2025 – Discussion started: 25 June 2025

Revised: 17 December 2025 – Accepted: 8 January 2026 – Published: 9 March 2026

Abstract. Coccolith dissolution in the water column is an important process in the marine carbon cycle. Identifying dissolution in water column samples has been difficult due to a lack of experimental reference datasets showing dissolution morphologies. We conducted a laboratory CaCO₃ dissolution experiment to detect differential dissolution morphologies of three selected coccolithophore (abundant marine calcareous phytoplankton) species, *Coccolithus braarudii*, *Helicosphaera carteri*, and *Scyphosphaera apsteinii*. These species were selected because they are ecologically and biogeochemically important (significant contributors to CaCO₃ production) and have been less studied than *Gephyrocapsa*. Murioliths of *S. apsteinii* dissolve faster than lopadoliths, which in turn dissolve as fast as *H. carteri* but faster than *C. braarudii*. In *S. apsteinii* lopadoliths, dissolution rate depends on the crystallographic orientation of the crystals. Comparison with field samples shows that experimental data are helpful when interpreting field samples. For example, we identify dissolution in water and sediment samples reported in the literature. In *C. braarudii* dissolution reveals a nanostructure on the proximal side of the distal shield, an observation that has implications for coccolith biomineralization models, which do not currently account for the formation of such a structure. This nanostructure features “units” of ca. 50–100 nm and resembles the nanostructure well known from extracellular calcifiers such as molluscs

and foraminifera. Whether this resemblance is underpinned by a similar formation mechanism remains unknown, but we think this unlikely.

Highlights.

- Experimental studies on biogenic CaCO₃ dissolution provide novel insights into field sample observations and biomineralization processes
- Experimental data aid the interpretation of aberrant coccolith morphology in field samples
- In *C. braarudii* partial dissolution reveals a nanostructure in the distal shield
- The nanostructure in *C. braarudii* requires adjustments in biomineralization models

1 Introduction

Present anthropogenic CO₂ concentration changes, both atmospheric and marine, cannot be fully understood without considering marine calcium carbonate, largely produced by calcifying organisms (Broecker and Peng, 1982; Morse and Mackenzie, 1990). These calcifying organisms influence air-sea CO₂ exchange in several ways, e.g. through particulate inorganic- and organic carbon production in the

surface ocean but also through export of calcium carbonate to the deep ocean (Morse and Mackenzie, 1990). The most productive marine calcium carbonate (CaCO_3) producers are pelagic organisms, with coccolithophores contributing ca. 90 % of global pelagic CaCO_3 production (Ziveri et al., 2023, 2025) and ca. 50 % of CaCO_3 sedimentation (Milliman, 1993; Broecker and Clark, 2009). Dissolution of CaCO_3 in the photic zone is an important process in the marine CaCO_3 cycle (Ziveri et al., 2023; Subhas et al., 2022; Sulpis et al., 2021). The importance of dissolution for the marine C-cycle has two main aspects. Firstly, dissolution of CaCO_3 releases two moles of alkalinity per one mole of dissolved inorganic carbon, thereby shifting the seawater C-system towards higher pH values (Zeebe and Wolf-Gladrow, 2001). Secondly, the loss of ballast minerals reduces carbon export efficiency thereby influencing the C-cycle long-term (Klaas and Archer, 2002). In addition to occurring in the open ocean photic zone, dissolution of carbonates in general, and coccoliths in particular, may also occur in sediments and coastal CO_2 vent sites (Honjo, 1975; Ziveri et al., 2014).

Assessing coccolith dissolution in these diverse settings can be challenging, but partial dissolution morphologies as identified in electron micrographs have proved a useful tool (e.g. Langer et al., 2007; Ziveri et al., 2014). Knowledge of such differential dissolution morphologies will aid interpretation of field samples, e.g. the degree of dissolution in one species will inform inferences about the degree of dissolution in other species. More fundamentally, knowledge about dissolution morphologies will enable us to accurately distinguish malformation/under-calcification from dissolution, which is not necessarily an easy task (Young, 1994). Finally, dissolution might reveal informative structural features (Langer et al., 2007). The main goal of our study is to provide a dissolution-morphology reference dataset which can be used to identify dissolution in water column samples. The applicability of our data to sediment samples might be more limited as discussed below. The interpretation of field samples is difficult, however, because the degree, and even the mere fact, of dissolution often need to be inferred from the micrographs alone, without precise knowledge of the physico-chemical conditions leading to the observed morphology. For example, in surface sediments *Calcidiscus leptoporus* coccoliths (placoliths characterized by two shield-like plates connected by a central tube) lacking proximal shields have been taken as a sign of heavy dissolution (Roth and Berger, 1975), which has been proposed as a proxy for dissolution in the sedimentary record (Matsuoka, 1990). Only an experimental study could show that separation of the shields is the first observable dissolution feature occurring at less than 8 % mass loss (Langer et al., 2007) revealing the “weak spot” at the proximal end of the tube (the position of the proto-coccolith ring, Young et al., 2004).

Despite the importance of experimental studies showing graded dissolution of coccoliths, only a few such studies have been conducted (McIntyre and McIntyre, 1971; Burns, 1977;

Kleijne, 1990; Henriksen et al., 2004; Langer et al., 2006a; Holcová and Scheiner, 2023), with a focus on *Gephyrocapsa* spp, in particular *G. huxleyi*, a widely used model species (Wheeler et al., 2023). The degree of dissolution in *G. huxleyi* water column samples is difficult to assess as there are variations of progressive dissolution patterns with e.g. warm- and cold-water phenotypes (Burns, 1977). The latter author pointed out that a tropical *G. huxleyi* loses the central grille in the first stages of dissolution, while a cold-water phenotype does not. Calcite removal from the long margin of the radial elements is a sign of early dissolution in the cold-water phenotype but not in a heavily calcified phenotype. These and similar observations made by Burns (1977) show that assessing the degree of dissolution in *G. huxleyi* is not an easy task and morphotype-specific assessments are required. While *G. huxleyi* is numerically the most abundant coccolithophore in present oceans, its contribution to coccolithophore CaCO_3 production is rivalled by some genera with larger coccoliths, such as *Calcidiscus* and *Coccolithus* (Wheeler et al., 2023). The relatively recent appearance of *G. huxleyi* in the fossil record implies that this species is not applicable to deep time sediment core studies (Henderiks et al., 2022). It is therefore worthwhile also studying genera with larger coccoliths and mass, biogeochemically important (Ziveri et al., 2004), and with a more extensive evolutionary history, e.g. *Coccolithus*, *Helicosphaera*, and *Scyphosphaera* (Henderiks et al., 2022). The latter genera are not as abundant as *G. huxleyi* but play an important role in coccolithophore CaCO_3 production and export in modern oceans (Baumann et al., 2004; Daniels et al., 2014, 2016; Gafar et al., 2019; Ziveri et al., 2007).

Based largely on field sediment studies, it is accepted that some coccolith forms dissolve faster than others. While *G. huxleyi* and *Umbilicosphaera sibogae* are among the fast-dissolving placolith bearing species, *G. oceanica*, *C. leptoporus*, and *C. pelagicus* are comparatively slow-dissolving (McIntyre and McIntyre, 1971; Berger, 1973; Roth and Coulbourn, 1982). These studies have not assessed how dissolution morphologies of different species relate to each other. In other words, which dissolution morphology of species x corresponds to a given dissolution morphology of species y?

Coccoliths contain crystals of different orientations, sizes, and shapes. A typical feature, for example, is the presence of crystals with radial *c*-axis orientations (R-units) and others with vertical *c*-axis orientations (V-units, Young et al., 1992). It might therefore be hypothesized that different crystals display different structural features, not only on the micrometre but also on the nanometre scale. Some of these features might only be discernible in partially dissolved specimens.

In this study we selected laboratory cultures of *Coccolithus braarudii*, *Helicosphaera carteri*, and *Scyphosphaera apsteinii*, and performed a dissolution experiment to follow their differential dissolution morphologies by means of sequential sampling for SEM analysis. Here we analyse two important aspects of dissolution. Firstly, the selective dissolution of different species relative to each other. Secondly, the

evolution of morphology of a given species with progressive dissolution. We hypothesize that dissolution morphologies will be different from malformations (Bianco et al., 2025; Langer et al., 2006b, 2021; Gerecht et al., 2015; Meyer et al., 2020) and therefore a dissolution reference dataset will enable us to unambiguously identify dissolution in field samples. The experimental setup chosen here is ideally suited to analyse sequential dissolution morphology with nanometric resolution. This enables the identification of different dissolution stages in field samples, providing additional information over and above the mere distinction of dissolution features and malformations.

Experimental dissolution studies provide a good source of information on the evolution of morphology with dissolution, without confounding factors from field studies such as variance in the primary biomineralization morphology.

2 Material and Methods

2.1 Culture conditions

Clonal cultures of *Coccolithus braarudii* (strain RCC1198), *Scyphosphaera apsteinii* (strain RCC3598), and *Helicosphaera carteri* (strain RCC1323) were grown in aged (3 months), sterile-filtered (Stericup-GP Sterile Vacuum Filtration System, 0.22 μm pore size, polyethersulfone membrane, Merck) natural surface seawater sampled in the English Channel off Roscoff, France, enriched with 288 μM nitrate, 18 μM phosphate, and silicate, trace metals, and vitamins as in Keller et al. (1987) with the following modifications: Cu and TRIS are omitted, $\text{NiCl}_2 \cdot 6\text{H}_2\text{O}$ 0.00314 μM is added, KH_2PO_4 is used as P source. All strains were obtained from the Roscoff Culture Collection (<http://www.roscoff-culture-collection.org>, last access: 12 February 2026).

Cultures were grown under a 16:8 h light:dark cycle at a light intensity of 50 $\mu\text{mol photons m}^{-2} \text{s}^{-1}$ in temperature-controlled culture incubators. *Coccolithus braarudii* RCC1198 was grown at 15 °C, while *Scyphosphaera apsteinii* RCC3598 and *Helicosphaera carteri* RCC1323 were grown at 20 °C. Cells were grown in dilute batch cultures, ensuring a quasi-constant seawater carbonate system over the course of exponential growth (Hoffmann et al., 2015). Cell densities were determined by flow cytometry immediately after sampling (Table S1 in the Supplement). Cultures used in the dissolution experiment were initially checked by light and scanning electron microscopy to ensure that coccosphere morphology was normal (as observed in light microscopy) and the percentage of coccolith malformations was below 15 % (as determined by SEM analysis, Langer and Bode, 2011). The latter is a very low percentage of malformations in cultures (in which values up to 90 % have been reported, Langer et al., 2006b; Langer et al., 2013), enabling this study to focus on normal coccoliths and

their dissolution morphologies, as opposed to the dissolution features of malformed coccoliths (Langer and Bode, 2011; Langer et al., 2013, 2023). We chose not to analyse the dissolution morphology of malformed coccoliths because results are intended to be applicable to field samples, in which the percentage of malformed coccoliths is typically only ca. 2 % (Langer et al., 2006b, 2013). Analysis of the dissolution morphologies of malformed coccoliths would require a different experimental setup, with cultures displaying high proportions of malformed coccoliths. Such an approach would be interesting in itself, but does not fall within the scope of the present study (Langer et al., 2006b).

2.2 Dissolution experiment

To study differential dissolution morphologies accurately, the selected species were combined in a single 2.7 L bottle (Holcová and Scheiner, 2023), in which case only one calcite saturation state (ω) value can be selected. In pre-experiments we found that *Gephyrocapsa huxleyi* coccoliths dissolved more than 10 \times faster than coccoliths of *Coccolithus braarudii*, *Helicosphaera carteri*, and *Scyphosphaera apsteinii*, meaning it was not possible to include *G. huxleyi* in our experiment. The three other species, *C. braarudii*, *H. carteri*, and *S. apsteinii*, displayed broadly similar dissolution kinetics and were therefore suited for our purpose.

To start the dissolution experiment, living cells were transferred into a 2.7 L bottle containing culture medium that was acidified using calculated amounts of HCl (3.29 M) immediately prior to cell transfer. We used acidification to manipulate ω calcite because it is more representative of dissolution scenarios in the field than changes in Ca concentration. ω calcite is the saturation state of seawater with respect to calcite, with $\omega < 1$ indicating dissolution and $\omega > 1$ potential crystal growth. This decision is important because the manipulation of ω calcite via acidification is more effective than via Ca concentration decrease (Hassenkam et al., 2011). We chose to work with living cells, as opposed to isolated coccoliths for the following reasons. Firstly, we wanted our results to be useful for comparison with various dissolution scenarios such as whole cells in copepod and micro-grazer guts, whole cells in marine snow aggregates, whole cells in ocean acidification-affected corrosive waters. Secondly, we wanted to analyse effects of dissolution on coccospheres, as opposed to only on individual coccoliths. Thirdly, removing coccoliths from cells is not always an easy task and often requires chemical or heat treatment which might alter structural integrity and organic content (Manuela Bordiga, personal communication, 2025). Since this is a pilot study, we wanted to keep the experimental setup as straightforward as possible. Follow up studies should deal with modified setups to explore additional factors influencing dissolution patterns. The culture medium prepared using natural surface seawater sampled off Roscoff, France has a typical dissolved inorganic carbon,

DIC, of ca. 2000 $\mu\text{mol kg}^{-1}$ (Johnson et al., 2022). We used this value for DIC and measured pH (NBS) = 6.44 to calculate ω calcite = 0.033 using the program CO2SYS (Pierrot et al., 2012). The calculated value for ω calcite (0.033) was therefore approximate (Table S2). However, DIC variability of natural surface seawater sampled off Roscoff, France is low, therefore introducing only a negligible inaccuracy in calculated ω calcite in the context of the present study, i.e. an error of ± 0.005 is expected (Johnson et al., 2022). The present study was not designed to analyse dissolution kinetics precisely (such as in Subhas et al., 2018), meaning an approximate determination of the carbonate system is sufficient. We used a Cyberscan 500 pH meter (Eutech Instruments, UK) equipped with a Mettler Toledo InLab 413/ID67 electrode to determine pH on the NBS scale.

Experimental dissolution over a very short space of time (on the order of seconds as in Yang et al., 2021) only allows for comparatively low-resolution light micrographs that would have been insufficient for our purpose. The advantage of a short experiment duration, however, is that DIC uptake and gas exchange with the atmosphere, and therefore carbonate system variability, is negligible. Our dissolution experiment, conducted over a duration of 11 h, was carried out in the dark at 4 °C to ensure that cellular metabolism (including photosynthesis and coccolith production) was severely restricted over the course of the experiment. Cell densities were 711 cells mL^{-1} for *C. braarudii*, 665 cells mL^{-1} for *H. carteri*, and 586 cells mL^{-1} for *S. apsteinii*. The resultant low overall cell density of 1963 cells mL^{-1} (Table S1) contributed to ensuring a quasi-constant carbonate system over the course of the experiment (Langer et al., 2006b; Langer and Bode, 2011; Hoffmann et al., 2015). Physico-chemical conditions over the course of the experiment were additionally homogenized by regular mixing, i.e. keeping the cells in suspension. No aggregation of cells occurred and no sedimentation of cells or coccoliths took place. The pH did rise by ca. 0.1 over the course of the experiment, but this corresponds to an increase in ω calcite of only ca. 0.005, i.e. the same magnitude as the minor uncertainty introduced by our choice of DIC value (see above).

After the dissolution experiment was completed, cells were transferred into normal culture conditions as specified above. All three species, *C. braarudii*, *H. carteri*, and *S. apsteinii*, resumed cell division and coccolith production as confirmed by optical inspection using light microscopy. We did not quantify coccolith morphology in re-calcifying cells, but noted that initially coccoliths seemed to display more malformations than prior to the dissolution experiment. This assessment is based on an informal analysis by means of light microscopy; no images were taken.

Multiple (15) sequential samples for detailed morphological analysis were taken over the 11 h duration of the experiment. Samples for SEM analysis were filtered onto polycarbonate filters (0.8 μm pore-size), dried in a drying cabinet at 50 °C for 24 h, then sputter-coated with gold–palladium

using a Cressington 108 sputter coater (Cressington Scientific Instruments, Watford, UK). Imaging was performed with a Phenom Pro desktop SEM at the Station Biologique de Roscoff, France, and an El SEM Zeiss Merlin at UAB, Barcelona, Spain. All the morphological features described in this study are discernible using the Phenom Pro desktop SEM. We used the Zeiss Merlin FE-SEM only to produce images showing the nanostructure on the proximal side of the distal shield of *C. braarudii* because the latter microscope has a higher resolution. This nanostructure, however, was discovered using the Phenom Pro desktop SEM. An average of ~ 350 coccoliths was analysed per sample (Langer and Benner, 2009). To describe dissolution morphologies, we selected conspicuous features that could be easily followed over the course of the experiment to ensure robust results and to facilitate application to field samples (Table S3). In *C. braarudii* and *H. carteri* we analysed dissolution features of coccospheres in addition to dissolution features of coccoliths. In *S. apsteinii* only dissolution features of coccoliths were analysed because coccospheres in this species lack the mechanical stability needed to consistently withstand the mechanical forces experienced in SEM preparation (Langer et al., 2023). The following morphological features were used to describe dissolution. In *C. braarudii*: (1) etching of the inner tube, (2) etching of the distal shield, (3) central area bar missing, (4) coccoliths broken, (5) gaps in coccospheres, (6) coccospheres collapsed, (7) nanostructure visible (on proximal side of distal shield). In *H. carteri*: (1) etching, (2) coccoliths broken, (3) coccospheres collapsed. In *S. apsteinii* lopadoliths: (1) etching of base, (2) etching of barrel, (3) rim serrated, (4) lopadoliths broken, (5) isolated lopadolith V units. In *S. apsteinii* muraloliths: (1) centre missing, (2) etching, (3) muraloliths broken (Table S3). Scanning electron micrographs of all of these features are shown in Figs. 1–5. The most important dissolution features for practical purposes are summarised in Table 1.

3 Results and Discussion

3.1 Differential dissolution: general observations

We subjected living cells of three common coccolithophore species, namely *Coccolithus braarudii*, *Helicosphaera carteri*, and *Scyphosphaera apsteinii*, to seawater undersaturated with respect to calcite, i.e. ω calcite ca. 0.033 (see Methods). The duration of the experiment was 11 hours, at the end of which only a few isolated distal shield elements of *C. braarudii* remained (Fig. 6). Our observation that *C. braarudii* is more dissolution resistant than *H. carteri* tallies well with conclusions drawn from studying Atlantic Ocean floor sediments (Berger, 1973). Information on *S. apsteinii* in differential dissolution studies is rare, with this species either only mentioned but not discussed or not mentioned at all (McIntyre and McIntyre, 1971; Berger, 1973; Roth and Coul-

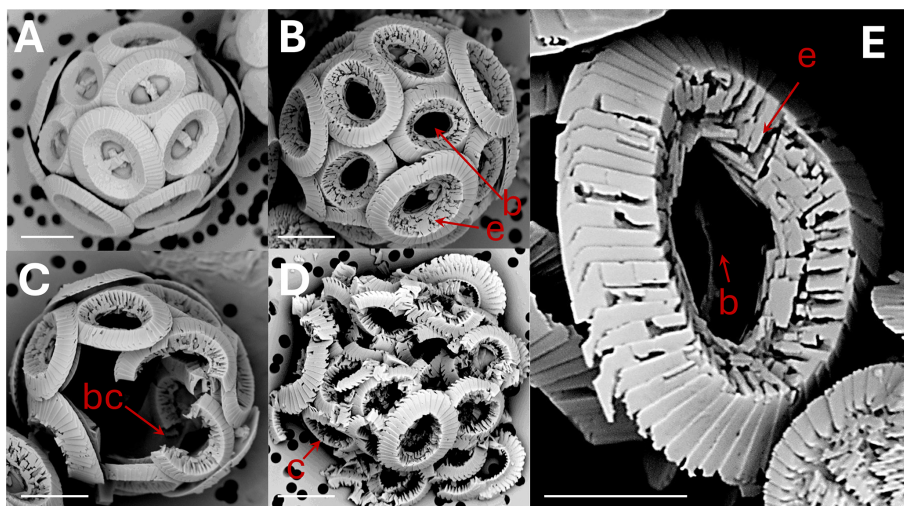


Figure 1. *Coccolithus braarudii*: (A) coccosphere at t_0 , no dissolution. Scale bar 5 μm . (B) coccosphere; etching (e) of tube and distal shield and central area bar missing (b). Scale bar 5 μm . (C) broken coccoliths (bc), etching of tube, central bar missing and gaps in coccosphere. Scale bar 5 μm . (D) collapsed coccosphere (c), also showing etching (e) of tube and distal shield and central area bar missing (b). Scale bar 5 μm . (E) coccolith, etching (e) of tube and distal shield, and central area bar missing (b). Note that the etching consistently occurs by opening of sutures between elements rather than by dissolution of element surfaces. Scale bar 3 μm .

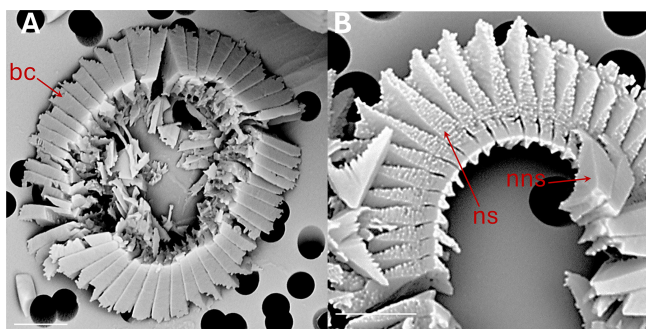


Figure 2. *Coccolithus braarudii*: (A) broken coccolith (bc) distal shield in distal view. (B) broken coccolith proximal view of distal shield showing nanostructure (ns); the arrow indicates isolated distal shield elements in distal view, from another coccolith, not displaying nanostructure (nns) on distal and vertical surfaces. All scale bars 2 μm .

bourne, 1982). From our data we conclude that *S. apsteinii* lopadoliths display dissolution kinetics similar to *H. carteri*, while *S. apsteinii* muroliths dissolve faster. In *S. apsteinii*, R-units, which are smaller and radially oriented, dissolve conspicuously faster than the larger, vertically oriented V-units (Figs. 6, 7, see also Drescher et al., 2012). Since lopadoliths contain calcite only, as opposed to e.g. aragonite (Walker et al., 2024), the latter observation illustrates that differential dissolution kinetics of biogenic calcium carbonate cannot be inferred from the polymorph only (Langer and Ziveri, 2025). Both etching and broken coccoliths appear simultaneously in *S. apsteinii* lopadoliths and *H. carteri* (Figs. 6, 7). In *C. braarudii* etching of the inner tube occurs simultaneously

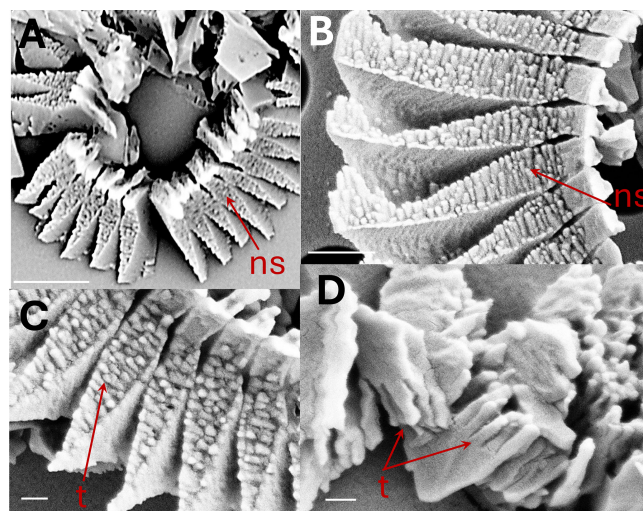


Figure 3. *Coccolithus braarudii*: (A) broken coccolith distal shield in proximal view showing nanostructure (ns). Scale bar 2 μm (B) proximal view of distal shield elements showing nanostructure (ns). Scale bar 500 nm. (C) proximal view of distal shield elements showing nanostructure (ns); individual “tubercles” (t) of the nanostructure are ca. 50–100 nm, Scale bar 200 nm. (D) isolated distal shield elements showing nanostructure “tubercles” (t) in vertical side view (arrow). Scale bar 200 nm.

with etching in *H. carteri* and *S. apsteinii*, but etching of the *C. braarudii* distal shield appears later, possibly because the latter features the largest crystals (Figs. 6, 7). Relatively slow dissolution of the distal shield compared to the tube/central

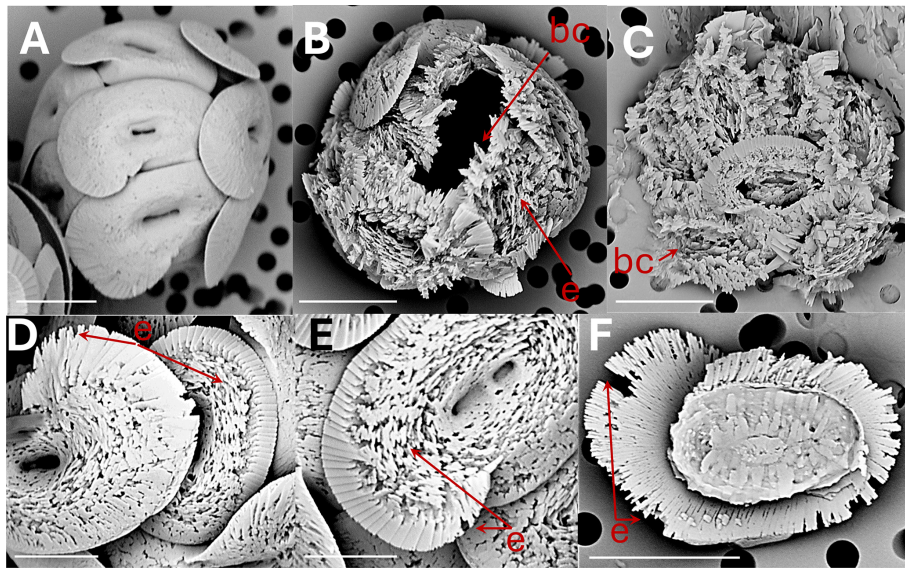


Figure 4. *Helicosphaera carteri*: (A) coccosphere at t_0 , no dissolution. Scale bar 5 μm . (B) coccosphere displaying coccoliths with severe etching (e) and a broken coccolith (bc). Scale bar 5 μm . (C) collapsed coccosphere including broken coccoliths (bc). Scale bar 5 μm . (D) coccoliths in distal view with etching (e) in flange and blanket. Scale bar 3 μm . (E) coccolith in distal view with etching in flange and blanket. Scale bar 2 μm . (F) coccolith in proximal view with etching (e) in flange. Scale bar 5 μm .

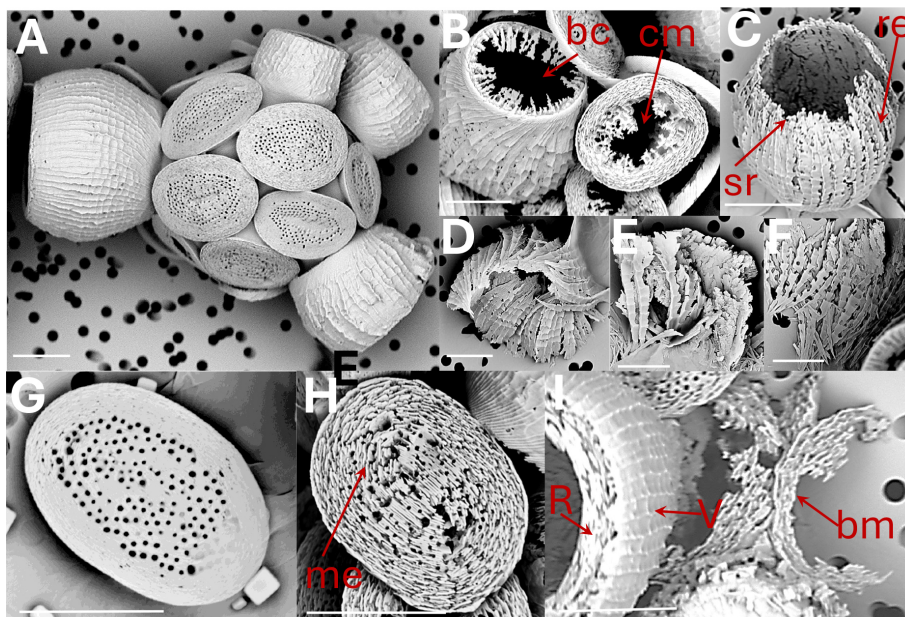


Figure 5. *Scyphosphaera apsteinii*: (A) coccosphere at t_0 , no dissolution (B) lopadolith base etching (be); murolith centre missing (cm) (C) lopadolith barrel etching (re) and serrated rim (sr) (D) and (E) broken lopadoliths (F) isolated V-units (G) murolith at t_0 , no dissolution (H) murolith with etching (me) (I) lopadolith in distal view showing R- and V-units (R- and V arrows, Young, 2008); and broken murolith (bm). All scale bars 5 μm .

area was also observed in *C. leptoporus* and might be a general feature of Coccolithales placoliths (Langer et al., 2007).

3.2 Comparison with field samples

3.2.1 Identification of dissolution in field samples

As noted in the introduction coccolith dissolution in the water column is being highlighted as a key process, greatly af-

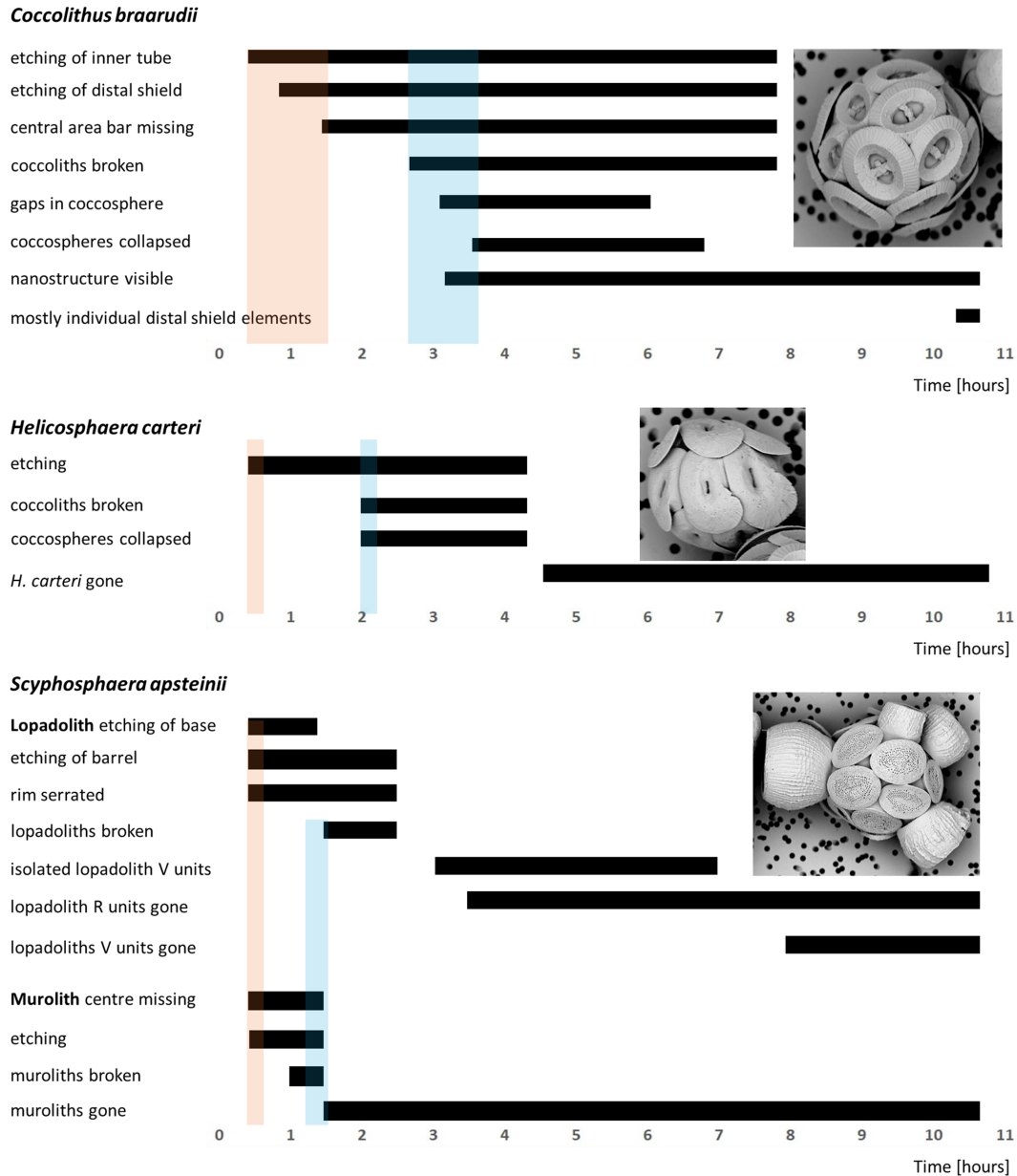


Figure 6. Timelines of dissolution. Bars indicate the period during which the respective feature can be observed. Shaded backgrounds indicate the onset points of major features. Pink backgrounds indicate the onset of etching, blue backgrounds indicate the onset of breakage/collapse. For example-images of each feature see Figs. 1–5.

fecting the export production of coccolith CaCO_3 to the bottom sediment. Our experimental results on the sequence of dissolution stages might usefully be applied to study of field samples in order to analyse and track water column dissolution. As a proof of concept we show here (Fig. 8) images of *Coccolithus braarudii* and *Helicosphaera carteri* coccoliths from sediment trap samples and of coccoliths from water column samples, in both cases showing dissolution features directly comparable to those we observed experimentally. It is also noteworthy that the nanostructure seen in the experimental samples is visible in the field samples (Fig. 8) show-

ing that it is not an experimental artefact. Comparable dissolution features have also been illustrated in the literature, for example by Cubillos et al. (2012) and Kleijne (1990), although in some cases they have been ascribed to malformation.

It is striking that in the three species studied here dissolution morphologies are clearly different from malformations. The latter do not resemble etching as described here (Figs. 1–5). This is remarkable considering that it has typically been difficult to distinguish dissolution from malformation, and even fracture, in *G. huxleyi* (McIntyre and McIntyre, 1971;

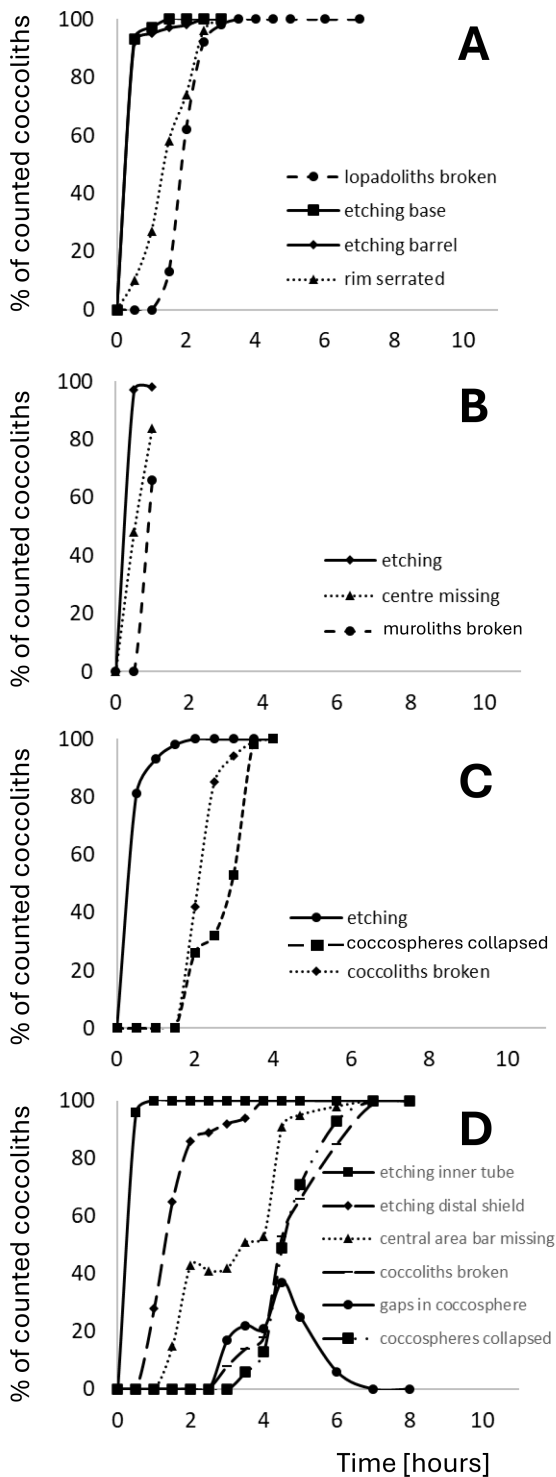


Figure 7. Quantification of the observations illustrated in Fig 6. Plotted is the percentage of each analysed feature versus time in hours from start of experiment. (A) *Scyphosphaera apsteinii* lopadoliths (B) *Scyphosphaera apsteinii* muraliths (C) *Helicosphaera carteri* (D) *Coccolithus braarudii*.

Table 1. Summary of important dissolution features.

Coccolith	Dissolution feature	Sketch
<i>C. braarudii</i>	Etching of inner tube	
<i>C. braarudii</i>	Etching of distal shield	
<i>C. braarudii</i>	Central area bar missing	
<i>H. carteri</i>	Etching	
<i>S. apsteinii</i> lopadoliths	Etching of barrel	
<i>S. apsteinii</i> lopadoliths	Serrated rim	
<i>S. apsteinii</i> muraliths	Etching	
<i>S. apsteinii</i> muraliths	Centre missing	

Burns, 1977; Kleijne, 1990; Holcová and Scheiner, 2023; Young, 1994, Langer et al., 2006b; Langer and Benner, 2009; Langer et al., 2011). These difficulties in identifying dissolution morphology in *G. huxleyi* are particularly conspicuous in morpho-type B/C, but are clearly noticeable in type A as well (own observations, unpublished). It might be speculated that dissolution is easier to identify in type R because the latter features fused distal shield elements which makes the overall morphology more similar to the one of the species studied here. This conjecture is supported by *G. huxleyi* morphotype-specific dissolution morphologies described in water column samples (Burns, 1977). It will be worthwhile studying different *G. huxleyi* morphotypes in greater detail. Species-specific dissolution features such as the serrated rim in *S. apsteinii* lopadoliths are also dissimilar to malformations such as type R (Langer et al., 2021; Langer et al., 2023). The nanostructure on the proximal side of the distal shield of *C. braarudii* is hardly visible in normal as well as malformed coccoliths,

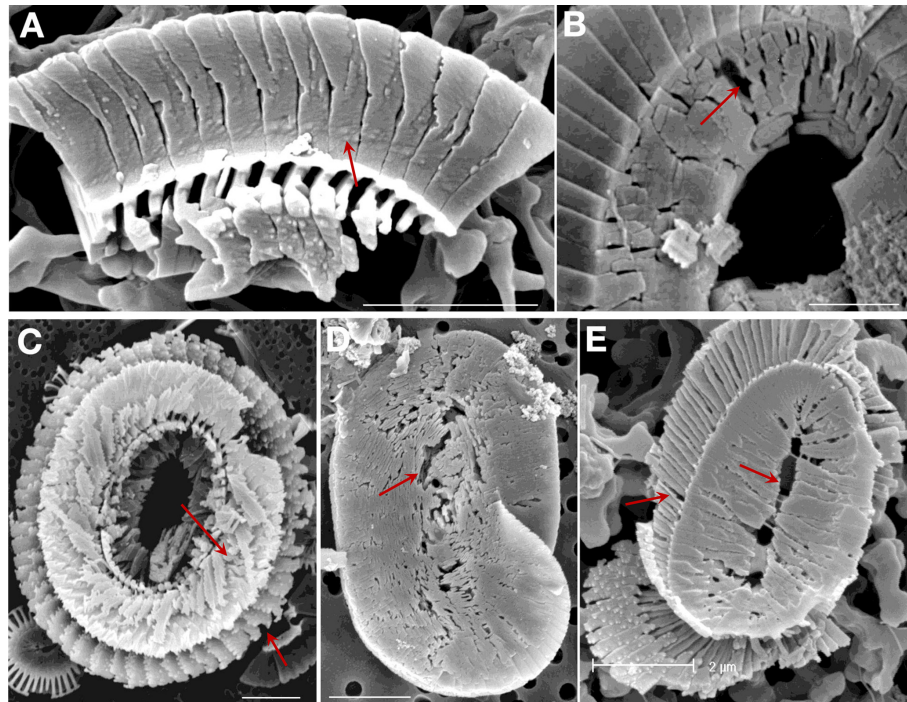


Figure 8. Field samples showing etching patterns comparable to those seen in the experimental samples (arrows). All scale bars 2 μm . *Coccolithus braarudii*: (A) Lower surface of a broken piece of distal shield showing nanostructure. (B) Central area of distal shield showing early stage dissolution. (C) Proximal surface showing advanced dissolution. *Helicosphaera carteri*: (D) Distal Surface showing early stage dissolution. (E) Proximal surface showing advanced dissolution. (A, B) sediment trap samples from 3200 m, N. Atlantic; (C) surface water sample, NW Atlantic; (D) – sediment trap sample, Canaries, 200 m; (E) plankton sample from 120 m, Gulf of Mexico.

whereas it is clearly visible in partially dissolved coccoliths. In *C. braarudii* a concentric hole sometimes appears in malformed coccoliths (Langer et al., 2021). This hole is clearly different from etch pits. A typical feature of more severe malformations in placolith bearing species is the distorted architecture of the shields (Bianco et al., 2025; Langer et al., 2006b; Langer and Benner, 2009; Langer et al., 2011; Langer and Bode, 2011; Langer et al., 2012; Langer et al., 2013, 2021, 2023; Kottmeier et al., 2022; Gerecht et al., 2015; Milner et al., 2016; Johnson et al., 2022) which does not occur as a result of dissolution.

3.2.2 Do the conditions under which dissolution occurs influence dissolution morphologies?

As a caveat we will say that dissolution morphologies might well depend on the conditions under which dissolution occurs. For example, the presence or absence of an organic coating around coccoliths results in slightly different dissolution morphologies as seen in high resolution AFM imaging (Henriksen et al., 2004). Since we did not remove the organic coating, our results should be best applicable to water samples (with organic coating) as opposed to sediment samples (in which the organic coating might be degraded). That said, the organic coating of coccoliths can still slow down dissolution after 70 Ma in the sediment (Sand et al., 2014).

Whether dissolution morphologies of these ancient coccoliths would be similar to those of cultured specimens remains to be tested. A good candidate would be *C. pelagicus* because it first appeared in the fossil record more than 60 Ma (Henderiks et al., 2022). Another aspect to consider is the way undersaturation is achieved. Dissolution kinetics in low-Ca solutions are different from those in low-pH solutions (Hasenkam et al., 2011). It is an open question whether dissolution morphologies would differ too. In addition, pressure-driven undersaturation might be relevant for deep-sea sediment samples. All of these issues are amenable to experimental testing and should be the focus of future studies.

3.3 Structural integrity of the coccosphere

An interesting difference between *C. leptoporus* (Langer et al., 2007) on the one hand and *C. braarudii*/*H. carteri* (this study) on the other hand is the structural integrity of coccospheres under dissolution. The earliest feature of dissolution in *C. leptoporus* dissolved at an omega calcite of 0.5, is the separation of the shields resulting in coccosphere collapse (Langer et al., 2007). By contrast, in *C. braarudii* and *H. carteri* the earliest dissolution feature is etching leaving the coccospheres intact. Only when coccoliths break due to more pronounced etching do coccospheres collapse in these species (Fig. 7). This means that living *C. leptoporus* cells

are more vulnerable to dissolution than *C. braarudii*/*H. carteri* because all three species need a coccosphere to live (Walker et al., 2018a; Bianco et al., 2025). While a coccosphere comprised of coccoliths produced by the very cell itself is essential for survival in monospecific cultures of these species, mixed-species coccospheres in natural assemblages indicate that coccosphere integrity can be re-established or modified through incorporation of foreign coccoliths (Johns et al., 2023). This might mean that a coccosphere compromised through dissolution or malformation might be repaired by incorporating foreign coccoliths. The protective efficacy of such hybrid coccospheres remains to be tested experimentally. However, the vulnerability sequence described above differs from what would be expected based on species specific coccolith solubility as inferred from sediment samples, which do not suggest that *C. leptoporus* is more vulnerable than *H. carteri* (Berger, 1973). Note that we cannot be entirely sure that *C. leptoporus* coccoliths would break faster than *H. carteri* coccoliths when subjected to the same omega calcite because the *C. leptoporus* experiment was conducted at an omega calcite of 0.5 (Langer et al., 2007) as opposed to the ca. 0.033 used here. Nevertheless, considering the very early appearance of separated shields in *C. leptoporus* (Langer et al., 2007) and the comparatively late appearance of broken coccoliths in *H. carteri*, it is highly likely that coccosphere collapse in *C. leptoporus* would occur earlier than in *H. carteri* (at a given omega calcite). Although bulk surface waters in most parts of the global ocean are currently supersaturated with respect to calcite, ongoing ocean acidification drives the calcite saturation state towards undersaturation which will be reached in some areas, e.g. the Southern Ocean, around the year 2100, posing a threat to calcifying organisms including coccolithophores (Langer and Ziveri, 2025). Please note that most surface waters will remain supersaturated with respect to calcite, so that our results are most directly relevant to locally undersaturated conditions (e.g. upwelling regions, eddies, sea-ice melt, or pore waters). Regardless of the actual threat posed by corrosive waters to living coccolithophores, the argument we are making here centres on relative vulnerability of different species in case of calcite undersaturation.

3.4 A nanostructure in *C. braarudii* biomineral

A nanostructure on the proximal side of the distal shield in *C. braarudii* became visible 3 h into the experiment (Fig. 6). The individual “units” of this nanostructure are ca. 50–100 nm in diameter. The distal side of the distal shield does not show this nanostructure. Differences between the proximal and distal sides of the distal shield have previously been reported (Henriksen et al., 2004; Young et al., 2004). Whereas the distal side of the distal shield consists of crystallographic a-faces, the proximal side seems to be more profoundly regulated by the cell and does not show crystallographic faces (Young et al., 2004). The nanostructure shown

here is what was described as “tuberculate surface” by Henriksen et al. (2004). The latter authors conclude that the tubercles are part of the calcite structure. We confirm this conclusion which is illustrated particularly well by a side view of these tubercles (Fig. 3D). We can only speculate what effect this nanostructure might have on the dissolution resistance/susceptibility of the distal shield elements. Considering that the distal shield elements of *C. braarudii* are the only coccolith parts of all three species that are still present at the end of the experiment (Fig. 6), it seems clear that they are comparatively dissolution resistant. Whether this resistance stems from the nanostructure or some other feature remains an open question but it is fair to say that the nanostructure does not make coccolith crystals highly susceptible to dissolution. The importance of micro- and nanostructures in differential dissolution behaviour of various biominerals has been recently highlighted in the context of vulnerability to ocean acidification (Langer and Ziveri, 2025). It is conceivable that the nanostructure in *C. braarudii* slows down etching and / or provides structural reinforcement. This scenario would be plausible if the nanostructure was an organo-mineral composite structure as opposed to being composed of calcite only (Walker and Langer, 2021). A nanostructure of similar size in CaCO_3 biominerals is widespread in extracellular calcifiers, where it is a central indicator of a layered growth mechanism featuring particle accretion which is believed to be non-operative in coccolithophores (Kadan et al., 2021; Walker and Langer, 2021). It remains, however, an open question whether the nanostructure in *C. braarudii* is similar to that in extracellular calcifiers i.e. whether it is also an organo-mineral composite structure (Walker and Langer, 2021). This question is pertinent to coccolithophore biomineralization because an extracellular-like nanostructure in coccoliths would call into question widely held views about crystallization of coccolith crystals (Walker and Langer, 2021). However, even if the tuberculate nanostructure in *C. braarudii* should turn out to be extracellular-like, it would still be unclear how it is possible that the distal side of the distal shield is different, i.e. shows crystallographic a-faces and no nanostructure. The standard biomineralization model explaining the nanostructure in extracellular calcifiers cannot account for the difference between the two sides of the distal shield in *C. braarudii*, and neither can the standard model of coccolith biomineralization (Young et al., 2004; Walker and Langer, 2021). This difference between the proximal and the distal side of the distal shield shows how finely tuned morphogenesis in *C. braarudii* is. We can only speculate how this fine tuning is achieved, but the composition of the organic coating might play a role. The composition of coccolith associated polysaccharides is known to be species specific, but we speculate that it might also be site specific within the coccolith vesicle (Walker et al., 2018b).

4 Conclusions

In summary, our results show that dissolution experiments complement field studies and contribute to a deeper understanding of both coccolith structure and the ecological impact of seawater undersaturation with respect to calcite. We conclude that

1. the most dissolution-resistant species is *C. braarudii*, followed by *H. carteri* and *S. apsteinii*;
2. structural integrity of the coccosphere under dissolution is highest in *C. braarudii*, followed by *H. carteri* and *S. apsteinii*, with *C. leptoporus* probably showing the weakest coccosphere;
3. we identify dissolution in published field data where it was not recognised;
4. lopadolith R-units dissolve faster than V-units, illustrating that different microstructures in the same coccolith have different dissolution kinetics despite containing the same mineral;
5. the nanostructure in the distal shield of *C. braarudii* points to a fine-tuning in coccolith morphogenesis that is not accounted for by our current model of coccolith biomineralization.

Data availability. All data are available in the Supplement.

Supplement. The supplement related to this article is available online at <https://doi.org/10.5194/bg-23-1795-2026-supplement>.

Author contributions. GL: conception, experiments, analysis, writing, IP: experiments, writing, JRY: analysis, field samples, writing, PZ: writing.

Competing interests. The contact author has declared that none of the authors has any competing interests.

Disclaimer. Publisher's note: Copernicus Publications remains neutral with regard to jurisdictional claims made in the text, published maps, institutional affiliations, or any other geographical representation in this paper. The authors bear the ultimate responsibility for providing appropriate place names. Views expressed in the text are those of the authors and do not necessarily reflect the views of the publisher.

Acknowledgements. We thank Martin Gachenot for technical assistance.

Financial support. Generalitat de Catalunya (MERS, 2021 SGR00640), Spanish Ministry of Science and Innovation (CEX2019-000940-M), and BIOCAL project (PID2020-113526RB-I00, Spanish Ministry of Science and Innovation). DFG project BONITOS 541693727.

Review statement. This paper was edited by Tina Treude and reviewed by two anonymous referees.

References

- Baumann, K.-H., Böckel, B., and Frenz, M.: Coccolith contribution to South Atlantic carbonate sedimentation, in: Coccolithophores, edited by: Thierstein, H. R. and Young, J. R., Springer Berlin Heidelberg, Berlin, Heidelberg, 367–402, https://doi.org/10.1007/978-3-662-06278-4_14, 2004.
- Berger, W. H.: Deep-sea carbonates: evidence for a coccolith lysocline, *Deep Sea Research and Oceanographic Abstracts*, 20, 917–921, [https://doi.org/10.1016/0011-7471\(73\)90110-1](https://doi.org/10.1016/0011-7471(73)90110-1), 1973.
- Bianco, S., Bordiga, M., Langer, G., Ziveri, P., Cerino, F., Di Giulio, A., and Lupi, C.: Low sensitivity of a heavily calcified coccolithophore under increasing CO₂: the case study of *Helicosphaera carteri*, *Biogeosciences*, 22, 1821–1837, <https://doi.org/10.5194/bg-22-1821-2025>, 2025.
- Broecker, W. and Clark, E.: Ratio of coccolith CaCO₃ to foraminifera CaCO₃ in late Holocene deep sea sediments, *Paleoceanography*, 24, 2009PA001731, <https://doi.org/10.1029/2009PA001731>, 2009.
- Broecker, W. S. and Peng, T.-H.: *Tracers in the Sea*, Lamont-Doherty Geological Observatory, Columbia University, 690 pp., ISBN 978-9993186724, 1982.
- Burns, D. A.: Phenotypes and dissolution morphotypes of the genus *Gephyrocapsa* kamptner and *Emiliania huxleyi* (Lohmann), *New Zealand Journal of Geology and Geophysics*, 20, 143–155, <https://doi.org/10.1080/00288306.1977.10431596>, 1977.
- Cubillos, J. C., Henderiks, J., Beaufort, L., Howard, W. R., and Hallegraef, G. M.: Reconstructing calcification in ancient coccolithophores: Individual coccolith weight and morphology of *Coccolithus pelagicus* (sensu lato), *Marine Micropaleontology*, 92–93, 29–39, <https://doi.org/10.1016/j.marmicro.2012.04.005>, 2012.
- Daniels, C., Poulton, A., Young, J., Esposito, M., Humphreys, M., Ribas-Ribas, M., Tynan, E., and Tyrrell, T.: Species-specific calcite production reveals *Coccolithus pelagicus* as the key calcifier in the Arctic Ocean, *Mar. Ecol. Prog. Ser.*, 555, 29–47, <https://doi.org/10.3354/meps11820>, 2016.
- Daniels, C. J., Sheward, R. M., and Poulton, A. J.: Biogeochemical implications of comparative growth rates of *Emiliania huxleyi* and *Coccolithus* species, *Biogeosciences*, 11, 6915–6925, <https://doi.org/10.5194/bg-11-6915-2014>, 2014.
- Drescher, B., Dillaman, R. M., and Taylor, A. R.: Coccolithogenesis in *S cyphosphaera apsteinii* (*Prymnesiophyceae*), *Journal of Phycology*, 48, 1343–1361, <https://doi.org/10.1111/j.1529-8817.2012.01227.x>, 2012.
- Gafar, N. A., Eyre, B. D., and Schulz, K. G.: Particulate inorganic to organic carbon production as a predictor for coccolithophorid

- sensitivity to ongoing ocean acidification, *Limnol. Oceanogr. Letters*, 4, 62–70, <https://doi.org/10.1002/lo12.10105>, 2019.
- Gerecht, A. C., Šupraha, L., Edvardsen, B., Langer, G., and Henderiks, J.: Phosphorus availability modifies carbon production in *Coccolithus pelagicus* (Haptophyta), *Journal of Experimental Marine Biology and Ecology*, 472, 24–31, <https://doi.org/10.1016/j.jembe.2015.06.019>, 2015.
- Hassenkam, T., Johnsson, A., Bechgaard, K., and Stipp, S. L. S.: Tracking single coccolith dissolution with picogram resolution and implications for CO₂ sequestration and ocean acidification, *Proc. Natl. Acad. Sci. U.S.A.*, 108, 8571–8576, <https://doi.org/10.1073/pnas.1009447108>, 2011.
- Henderiks, J., Sturm, D., Šupraha, L., and Langer, G.: Evolutionary Rates in the Haptophyta: Exploring Molecular and Phenotypic Diversity, *JMSE*, 10, 798, <https://doi.org/10.3390/jmse10060798>, 2022.
- Henriksen, K., Young, J. R., Bown, P. R., and Stipp, S. L. S.: Coccolith biomineralisation studied with atomic force microscopy, *Palaeontology*, 47, 725–743, <https://doi.org/10.1111/j.0031-0239.2004.00385.x>, 2004.
- Hoffmann, R., Kirchlechner, C., Langer, G., Wochnik, A. S., Griesshaber, E., Schmahl, W. W., and Scheu, C.: Insight into *Emiliania huxleyi* coccospheres by focused ion beam sectioning, *Biogeosciences*, 12, 825–834, <https://doi.org/10.5194/bg-12-825-2015>, 2015.
- Holcová, K. and Scheiner, F.: An experimental study on post-mortem dissolution and overgrowth processes affecting coccolith assemblages: A rapid and complex process, *Geobiology*, 21, 193–209, <https://doi.org/10.1111/gbi.12528>, 2023.
- Honjo, S.: Dissolution of suspended coccoliths in the deep-sea water column and sedimentation of coccolith ooze, in: *Dissolution of Deep-sea Carbonates*, Sliter, W.V., Bé, A.W.H., Berger, W.H., ISBN 978-1-970168-07-5, 1975.
- Johns, C. T., Bondoc-Naumovitz, K. G., Matthews, A., Matson, P. G., Iglesias-Rodriguez, M. D., Taylor, A. R., Fuchs, H. L., and Bidle, K. D.: Adsorptive exchange of coccolith biominerals facilitates viral infection, *Sci. Adv.*, 9, eadc8728, <https://doi.org/10.1126/sciadv.adc8728>, 2023.
- Johnson, R., Langer, G., Rossi, S., Probert, I., Mammone, M., and Ziveri, P.: Nutritional response of a coccolithophore to changing PH and temperature, *Limnology & Oceanography*, 67, 2309–2324, <https://doi.org/10.1002/lno.12204>, 2022.
- Kadan, Y., Tollervey, F., Varsano, N., Mahamid, J., and Gal, A.: Intracellular nanoscale architecture as a master regulator of calcium carbonate crystallization in marine microalgae, *Proc. Natl. Acad. Sci. U.S.A.*, 118, e2025670118, <https://doi.org/10.1073/pnas.2025670118>, 2021.
- Keller, M. D., Selvin, R. C., Claus, W., and Guillard, R. R. L.: MEDIA FOR THE CULTURE OF OCEANIC ULTRAPHYTOPLANKTON1,2, *Journal of Phycology*, 23, 633–638, <https://doi.org/10.1111/j.1529-8817.1987.tb04217.x>, 1987.
- Klaas, C. and Archer, D. E.: Association of sinking organic matter with various types of mineral ballast in the deep sea: Implications for the rain ratio, *Global Biogeochem. Cy.*, 16, <https://doi.org/10.1029/2001GB001765>, 2002.
- Kleijne, A.: Distribution and malformation of extant calcareous nannoplankton in the Indonesian Seas, *Marine Micropaleontology*, 16, 293–316, [https://doi.org/10.1016/0377-8398\(90\)90008-A](https://doi.org/10.1016/0377-8398(90)90008-A), 1990.
- Kottmeier, D. M., Chrachri, A., Langer, G., Helliwell, K. E., Wheeler, G. L., and Brownlee, C.: Reduced H⁺ channel activity disrupts pH homeostasis and calcification in coccolithophores at low ocean pH, *P. Natl. Acad. Sci. USA*, 119, e2118009119, <https://doi.org/10.1073/pnas.2118009119>, 2022.
- Langer, G. and Benner, I.: Effect of elevated nitrate concentration on calcification in *Emiliania huxleyi*, *J. Nannoplankton Res.*, 30, 77–82, <https://doi.org/10.58998/jnr2158>, 2009.
- Langer, G. and Bode, M.: CO₂ mediation of adverse effects of seawater acidification in *Calcidiscus leptoporus*, *Geochem. Geophys. Geosyst.*, 12, 2010GC003393, <https://doi.org/10.1029/2010GC003393>, 2011.
- Langer, G. and Ziveri, P.: Vulnerability to ocean acidification of marine calcifying organisms cannot be predicted from the mineral type in their shells, *Limnol. Oceanogr. Letters*, 10, 448–452, <https://doi.org/10.1002/lo12.70020>, 2025.
- Langer, G., Gussone, N., Nehrke, G., Riebesell, U., Eisenhauer, A., Kuhnert, H., Rost, B., Trimborn, S., and Thoms, S.: Coccolith strontium to calcium ratios in *Emiliania huxleyi*: The dependence on seawater strontium and calcium concentrations, *Limnol. Oceanogr.*, 51, 310–320, <https://doi.org/10.4319/lo.2006.51.1.0310>, 2006a.
- Langer, G., Geisen, M., Baumann, K., Kläs, J., Riebesell, U., Thoms, S., and Young, J. R.: Species-specific responses of calcifying algae to changing seawater carbonate chemistry, *Geochem. Geophys. Geosyst.*, 7, 2005GC001227, <https://doi.org/10.1029/2005GC001227>, 2006b.
- Langer, G., Nehrke, G., and Jansen, S.: Dissolution of *Calcidiscus leptoporus* coccoliths in copepod guts? A morphological study, *Mar. Ecol. Prog. Ser.*, 331, 139–146, <https://doi.org/10.3354/meps331139>, 2007.
- Langer, G., Probert, I., Nehrke, G., and Ziveri, P.: The morphological response of *Emiliania huxleyi* to seawater carbonate chemistry changes: an inter-strain comparison, *Journal of Nannoplankton Research*, 32, 29–34, 2011.
- Langer, G., Oetjen, K., and Brenneis, T.: Calcification of *Calcidiscus leptoporus* under nitrogen and phosphorus limitation, *J. Exp. Mar. Biol. Ecol.*, 413, 131–137, <https://doi.org/10.1016/j.jembe.2011.11.028>, 2012.
- Langer, G., Oetjen, K., and Brenneis, T.: On culture artefacts in coccolith morphology, *Helgol. Mar. Res.*, 67, 359–369, <https://doi.org/10.1007/s10152-012-0328-x>, 2013.
- Langer, G., Taylor, A. R., Walker, C. E., Meyer, E. M., Ben Joseph, O., Gal, A., Harper, G. M., Probert, I., Brownlee, C., and Wheeler, G. L.: Role of silicon in the development of complex crystal shapes in coccolithophores, *New Phytologist*, 231, 1845–1857, <https://doi.org/10.1111/nph.17230>, 2021.
- Langer, G., Probert, I., Cox, M. B., Taylor, A., Harper, G. M., Brownlee, C., and Wheeler, G.: The Effect of cytoskeleton inhibitors on coccolith morphology in *Coccolithus braarudii* and *Scyphosphaera apsteinii*, *Journal of Phycology*, 59, 87–96, <https://doi.org/10.1111/jpy.13303>, 2023.
- Matsuoka, H.: A new method to evaluate dissolution of CaCO₃ in the deep-sea sediments, *Transactions and proceedings of the Paleontological Society of Japan*, The Paleontological Society of Japan, 430–434, https://doi.org/10.14825/prpsj1951.1990.157_430, 1990.
- McIntyre, A. and McIntyre, R.: Coccolith concentration and differential solution in oceanic sediments, in: *The micropaleontology*

- of oceans, Cambridge University Press, Cambridge, 253–261, ISBN 9780521187480, 1971.
- Meyer, E. M., Langer, G., Brownlee, C., Wheeler, G. L., and Taylor, A. R.: Sr in coccoliths of *Scyphosphaera apsteinii*: Partitioning behavior and role in coccolith morphogenesis, *Geochimica et Cosmochimica Acta*, 285, 41–54, <https://doi.org/10.1016/j.gca.2020.06.023>, 2020.
- Milliman, J. D.: Production and accumulation of calcium carbonate in the ocean: Budget of a nonsteady state, *Global Biogeochemical Cycles*, 7, 927–957, <https://doi.org/10.1029/93GB02524>, 1993.
- Milner, S., Langer, G., Grelaud, M., and Ziveri, P.: Ocean warming modulates the effects of acidification on *Emiliana huxleyi* calcification and sinking, *Limnol. Oceanogr.*, 61, 1322–1336, <https://doi.org/10.1002/lno.10292>, 2016.
- Morse, J. and Mackenzie, F.: *Geochemistry of sedimentary carbonates*, Elsevier, ISBN 978-0-444-88781-8, 1990.
- Pierrot, D., Lewis, E., and Wallace, D. W. R.: MS Excel Program Developed for CO₂ System Calculations, ORNL Environmental Sciences Division, https://doi.org/10.3334/CDIAC/otg.CO2SYS_XLS_CDIAC105a, 2012.
- Roth, P. and Berger, W.: Distribution and dissolution of coccoliths in the south and central Pacific, in: *CaCO₃ dissolution in the deep sea*, Cushman Foundation for Foraminiferal Research, Santa Barbara, CA, 87–113, ISBN 9781970168075, 1975.
- Roth, P. H. and Coulbourn, W. T.: Floral and solution patterns of coccoliths in surface sediments of the North Pacific, *Marine Micropaleontology*, 7, 1–52, [https://doi.org/10.1016/0377-8398\(82\)90014-7](https://doi.org/10.1016/0377-8398(82)90014-7), 1982.
- Sand, K. K., Pedersen, C. S., Sjöberg, S., Nielsen, J. W., Makovicky, E., and Stipp, S. L. S.: Biomineralization: Long-Term Effectiveness of Polysaccharides on the Growth and Dissolution of Calcite, *Crystal Growth & Design*, 14, 5486–5494, <https://doi.org/10.1021/cg5006743>, 2014.
- Subhas, A. V., Rollins, N. E., Berelson, W. M., Erez, J., Ziveri, P., Langer, G., and Adkins, J. F.: The dissolution behavior of biogenic calcites in seawater and a possible role for magnesium and organic carbon, *Marine Chemistry*, 205, 100–112, <https://doi.org/10.1016/j.marchem.2018.08.001>, 2018.
- Subhas, A. V., Dong, S., Naviaux, J. D., Rollins, N. E., Ziveri, P., Gray, W., Rae, J. W. B., Liu, X., Byrne, R. H., Chen, S., Moore, C., Martell-Bonet, L., Steiner, Z., Antler, G., Hu, H., Lunstrum, A., Hou, Y., Kemnitz, N., Stutsman, J., Pallacks, S., Dugenne, M., Quay, P. D., Berelson, W. M., and Adkins, J. F.: Shallow Calcium Carbonate Cycling in the North Pacific Ocean, *Global Biogeochemical Cycles*, 36, e2022GB007388, <https://doi.org/10.1029/2022GB007388>, 2022.
- Sulpis, O., Jeansson, E., Dinauer, A., Lauvset, S. K., and Middelburg, J. J.: Calcium carbonate dissolution patterns in the ocean, *Nat. Geosci.*, 14, 423–428, <https://doi.org/10.1038/s41561-021-00743-y>, 2021.
- Walker, C. E., Heath, S., Salmon, D. L., Smirnov, N., Langer, G., Taylor, A. R., Brownlee, C., and Wheeler, G. L.: An Extracellular Polysaccharide-Rich Organic Layer Contributes to Organization of the Cocosphere in Coccolithophores, *Front. Mar. Sci.*, 5, 306, <https://doi.org/10.3389/fmars.2018.00306>, 2018a.
- Walker, C. E., Taylor, A. R., Langer, G., Durak, G. M., Heath, S., Probert, I., Tyrrell, T., Brownlee, C., and Wheeler, G. L.: The requirement for calcification differs between ecologically important coccolithophore species, *New Phytologist*, 220, 147–162, <https://doi.org/10.1111/nph.15272>, 2018b.
- Walker, J. M. and Langer, G.: Coccolith crystals: Pure calcite or organic-mineral composite structures?, *Acta Biomaterialia*, 125, 83–89, <https://doi.org/10.1016/j.actbio.2021.02.025>, 2021.
- Walker, J. M., Greene, H. J. M., Moazzam, Y., Quinn, P. D., Parker, J. E., and Langer, G.: An uneven distribution of strontium in the coccolithophore *Scyphosphaera apsteinii* revealed by nanoscale X-ray fluorescence tomography, *Environ. Sci.: Processes Impacts*, 26, 966–974, <https://doi.org/10.1039/D3EM00509G>, 2024.
- Wheeler, G. L., Sturm, D., and Langer, G.: *Gephyrocapsa huxleyi (Emiliana huxleyi)* as a model system for coccolithophore biology, *Journal of Phycology*, 59, 1123–1129, <https://doi.org/10.1111/jpy.13404>, 2023.
- Yang, M., Batchelor-McAuley, C., Barton, S., Rickaby, R. E. M., Bouman, H. A., and Compton, R. G.: Opto-Electrochemical Dissolution Reveals Coccolith Calcium Carbonate Content, *Angew. Chem. Int. Ed.*, 60, 20999–21006, <https://doi.org/10.1002/anie.202108435>, 2021.
- Young, J. R.: Variation in *Emiliana huxleyi* coccolith morphology in samples from the Norwegian EHUX experiment, 1992, *Sarsia*, 79, 417–425, <https://doi.org/10.1080/00364827.1994.10413573>, 1994.
- Young, J. R.: *Scyphosphaera porosa* Kämtner 1967 rediscovered in the plankton., *J. Nannoplankton Res.*, 30, 35–38, <https://doi.org/10.58998/jnr2292>, 2008.
- Young, J. R., Didymus, J. M., Brown, P. R., Prins, B., and Mann, S.: Crystal assembly and phylogenetic evolution in heterococcoliths, *Nature*, 356, 516–518, <https://doi.org/10.1038/356516a0>, 1992.
- Young, J. R., Henriksen, K., and Probert, I.: Structure and morphogenesis of the coccoliths of the CODENET species, in: *Coccolithophores*, edited by: Thierstein, H. R. and Young, J. R., Springer Berlin Heidelberg, Berlin, Heidelberg, 191–216, https://doi.org/10.1007/978-3-662-06278-4_8, 2004.
- Zeebe, R. and Wolf-Gladrow, D.: *CO₂ in Seawater: Equilibrium, Kinetics, Isotopes*, Elsevier, Amsterdam, 346 pp., ISBN 9780444509468, 2001.
- Ziveri, P., Baumann, K.-H., Böckel, B., Bollmann, J., and Young, J.: Present day coccolithophore-biogeography in the Atlantic Ocean, in: *Coccolithophores: From Molecular Processes to Global Impact*, Springer Verlag, 403–428, ISBN 978-3-540-21928-6, 2004.
- Ziveri, P., De Bernardi, B., Baumann, K.-H., Stoll, H. M., and Mortyn, P. G.: Sinking of coccolith carbonate and potential contribution to organic carbon ballasting in the deep ocean, *Deep Sea Research Part II: Topical Studies in Oceanography*, 54, 659–675, <https://doi.org/10.1016/j.dsr2.2007.01.006>, 2007.
- Ziveri, P., Passaro, M., Incarbona, A., Milazzo, M., Rodolfo-Metalpa, R., and Hall-Spencer, J. M.: Decline in Coccolithophore Diversity and Impact on Coccolith Morphogenesis Along a Natural CO₂ Gradient, *The Biological Bulletin*, 226, 282–290, <https://doi.org/10.1086/BBLv226n3p282>, 2014.
- Ziveri, P., Gray, W. R., Anglada-Ortiz, G., Manno, C., Grelaud, M., Incarbona, A., Rae, J. W. B., Subhas, A. V., Pallacks, S., White, A., Adkins, J. F., and Berelson, W.: Pelagic calcium carbonate production and shallow dissolution in the North Pacific

Ocean, Nat. Commun., 14, 805, <https://doi.org/10.1038/s41467-023-36177-w>, 2023.

Ziveri, P., Langer, G., Chaabane, S., De Vries, J., Gray, W. R., Keul, N., Hatton, I. A., Manno, C., Norris, R., Pallacks, S., Young, J. R., Schiebel, R., Zarkogiannis, S., Anglada-Ortiz, G., Bianco, S., De Garidel-Thoron, T., Grelaud, M., Lucas, A., Probert, I., and Mortyn, P. G.: Calcifying plankton: From biomineralization to global change, *Science*, 390, eadq8520, <https://doi.org/10.1126/science.adq8520>, 2025.